analytical chemistry

Article

Cite This: *Anal. Chem.* 2018, 90, 2867−2874

pubs.acs.org/ac

Single Drop Whole Blood Diagnostics: Portable Biomedical Sensor for Cardiac Troponin I Detection

Indu Sarangadharan,[†] Shin-Li Wang,[†] Revathi Sukesan,[†] Pei-chi Chen,[†] Tze-Yu Dai,[†] Anil Kumar Pulikkathodi,[†] Chen-Pin Hsu,[†] Hui-Hua Kenny Chiang,[§] Lawrence Yu-Min Liu,*[,∥,⊥] and Yu-Lin Wang*[,†,‡]

[†]Institute of Nanoengineering and Microsystems, National Tsing Hua University, Hsinchu, 300, Taiwan R.O.C.

[‡]Department of Power Mechanical Engineering, National Tsing Hua University, Hsinchu, 300, Taiwan R.O.C.

[§]Department of Biomedical Engineering, National Yang Ming University, Taipei, 112, Taiwan R.O.C.

[∥]Division of Cardiology, Department of Internal Medicine, Mackay Memorial Hospital, Hsinchu, 300, Taiwan R.O.C.

[⊥]Department of Medical Science & Institute of Bioinformatics and Structural Biology, National Tsing Hua University, Hsinchu, 300, Taiwan R.O.C.

Supporting Information

ABSTRACT: Detection of disease biomarkers from whole blood is very important in disease prevention and management. However, new generation assays like point-of-care or mobile diagnostics face a myriad of challenges in detecting proteins from whole blood. In this research, we have designed, fabricated, and characterized a portable biomedical sensor for the detection of cardiac troponin I (cTnI) directly from whole blood, without sample pretreatments. The sensing methodology is based on an extended gate electrical double layer (EDL) gated field effect transistor (FET) biosensor that can offer very high sensitivity, a wide dynamic range, and high selectivity to target analyte. The sensing methodology is not impeded by electrostatic screening and can be applied to all types of FET sensors. A portable biomedical system is designed to carry out the diagnostic assay in a very simple and rapid manner, that allows the user to screen for target protein from a single drop of blood, in 5 min. This biomedical sensor can be used in hospitals and homes alike, for early detection of cTnI which is a clinical marker for acute myocardial infarction. This sensing methodology could potentially revolutionize the modern health care industry.

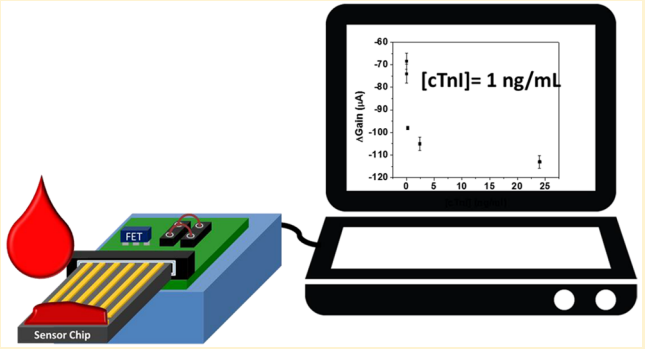

In recent years, there has been increased attention toward health monitoring systems, more importantly, cardiac monitoring through smart electronic gadgets and hospital-based tests such as electrocardiography (ECG) and hemodynamics.[1−4] However, health status information delivered via smart gadgets is not sufficient to diagnose or monitor underlying diseases. Hospital-based tests are labor intensive and cannot be performed at the comfort of homes or work places, which renders many people all around the world with inaccessibility to emergency medical attention. Cardiovascular diseases (CVDs) remain as the major cause of mortality all over the world, affecting developing economies more than the developed ones.[5,6] Molecular biomarkers have been reported to be highly efficient diagnostic and prognostic markers of CVDs, and clinicians have arrived at the consensus of using molecular cardiac biomarkers along with conventional biomarkers or indices such as age, medical history, and cholesterol levels, for better CVD risk assessment and prevention.[7,8] For example, the diagnosis and prognosis of acute myocardial infarction (AMI) is dependent on a blood test for cardiac troponin I (cTnI), a protein-based marker of cardiac muscle injury along with electrophysiology tests.[9,10] Currently, spectrophotometric methodologies such as ELISA, electrochemiluminiscence, immunoturbidimetry, and surface plasmon resonance (SPR) are used in hospitals to monitor MI in patients.[11−14] These tests can be performed only in hospitals or specialized diagnostic centers, requiring trained laboratory staff. They are also very expensive and time-consuming. The inaccessibility and unaffordable high prices of the current CVD diagnostics endangers the lives of millions of people all around the globe.

Field effect transistor (FET)-based biosensors have been considered as a highly sensitive and cost-effective diagnostic platform for the detection of several biological analytes ranging from nucleic acids to cellular targets.[15,16] Previously, several FET-based biosensors have been implemented using silicon nanostructures,[17] compound semiconductors,[18] and novel 2-

Received: December 3, 2017
Accepted: January 28, 2018
Published: January 29, 2018

DOI: 10.1021/acs.analchem.7b05018
Anal. Chem. 2018, 90, 2867−2874

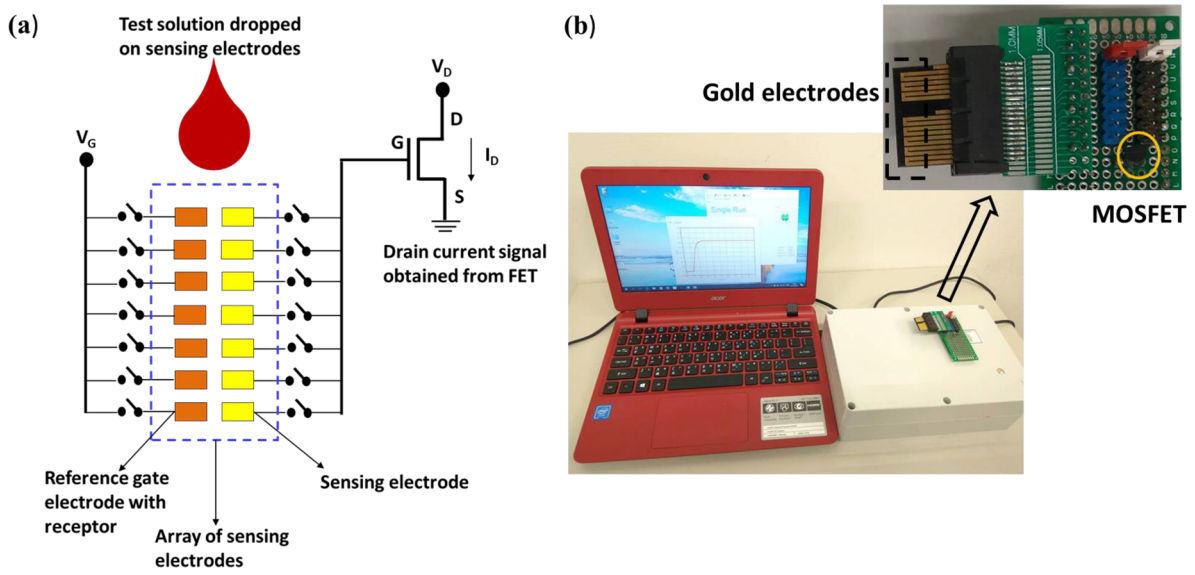

Figure 1. Structure and protocols of the extended gate EDL FET biosensor. (a) Schematic diagram of the extended gate EDL FET sensor. (b) Real image of the portable biosensor system interfaced with a laptop to display the results. Inset shows the sensor chip connected to the MOSFET.

dimensional materials.[19,20] However, the advancement of FET-based biosensors was hindered due to the phenomenon of the charge screening effect, which screens off the applied potential within the Debye length.[21,22] This restricted the use of FET-based biosensors to low electrolyte test samples which significantly affects the binding kinetics and integrity of biosamples.

Several methods have been proposed in the past to overcome the charge screening effect and apply FET-based biosensors to the detection of biomarkers in whole blood.[22−24] However, these methodologies require elaborate and complicated sample pretreatment methods such as repeated washing and enrichment, dilution, and desalting. These steps add to the complexity of the biosensing system yet do not ensure the physiological environment preservation to provide reliable biological signal acquisition. As a result, the sensing methodologies do not possess sufficient merit to counter the conventional laboratory-based spectroscopic techniques. Previously, we developed an electrical double layer (EDL) gated FET biosensor for the direct detection of target analytes in physiological salt concentration buffer (1× PBS) and human serum samples,[25] without extensive pretreatments or a washing process.

In this study, we have developed a portable biosensor system that can detect cTnI from a single drop of blood, in 5 min, in a minute fraction of the cost of current CVD diagnostics. We designed, fabricated, and characterized an extended gate EDL FET biosensor to detect cardiac troponin I (cTnI) from whole blood samples, without the use of extensive sample pretreatments such as dilution or desalting. The sensor exhibits high sensitivity, specificity, and wide dynamic range of detection in purified cTnI samples, whole blood spiked with cTnI, and clinical whole blood samples. If fresh whole blood samples (untreated) are being used, simple gravitational separation of blood cells can be employed by facing the sensor chip downward. It is also shown that gravitational separation of blood cells is not required if the whole blood samples have been treated with anticoagulant. Along with preserving the biosample integrity, we have simplified the whole cTnI assay format in such a way that, in a commercial biosensor system, the consumer would be able to perform the test with few assay protocols, requiring only 5 min of test duration and very low sample volume (<10 μL). These features enable our sensing methodology to be at par or transcend the benefits and utility of conventional diagnostics, with bright prospects in point of care and mobile diagnostic systems.

METHODS

The steps involved in sensor fabrication methods, sensor measurement (described in Figures S1 and S2), and sensor regeneration techniques are detailed in the Supporting Information.

Sensor Surface Functionalization. Monoclonal antibody (mAb) to cTnI is purchased from Hytest Inc. mAb and cysteamine hydrochloride are mixed together in the molar ratio of 10 000:1. The mixture is incubated for 15 min at 37 °C in a reaction tube followed by incubation on the sensor surface for 1.5 h in room temperature. The sensor is further incubated at 4 °C for 12 h after which unbound antibodies are washed away in PBS.

Purified cTnI Samples. Purified cTnI is purchased from Abcam and diluted to desired target concentrations in 1× PBS (pH 7.4, 150 mM NaCl, 10 mM PO_4^{3-}) containing 4% bovine serum albumin (BSA). BSA is added in the test solution to simulate the real conditions of blood serum samples.

Clinical cTnI Samples. The clinical whole blood samples are obtained from patients admitted to the hospital as per the IRB No. 16MMHIS112. The whole blood samples are collected from different individuals at different times, in a vacutainer treated with anticoagulant. The whole blood samples with undetected cTnI are collected from a healthy individual, in a vacutainer treated with anticoagulant, as per the IRB No. 10610HE074.

RESULTS

Figure 1 depicts the structure of extended gate EDL FET sensor. In each pair of gold electrodes, one electrode finger serves as the reference gate electrode which is biased with pulsed gate voltage V_g, and the other electrode finger serves as the sensing electrode which is connected to the gate terminal of the MOSFET. The schematic diagram of the extended gate

DOI: 10.1021/acs.analchem.7b05018
Anal. Chem. 2018, 90, 2867−2874

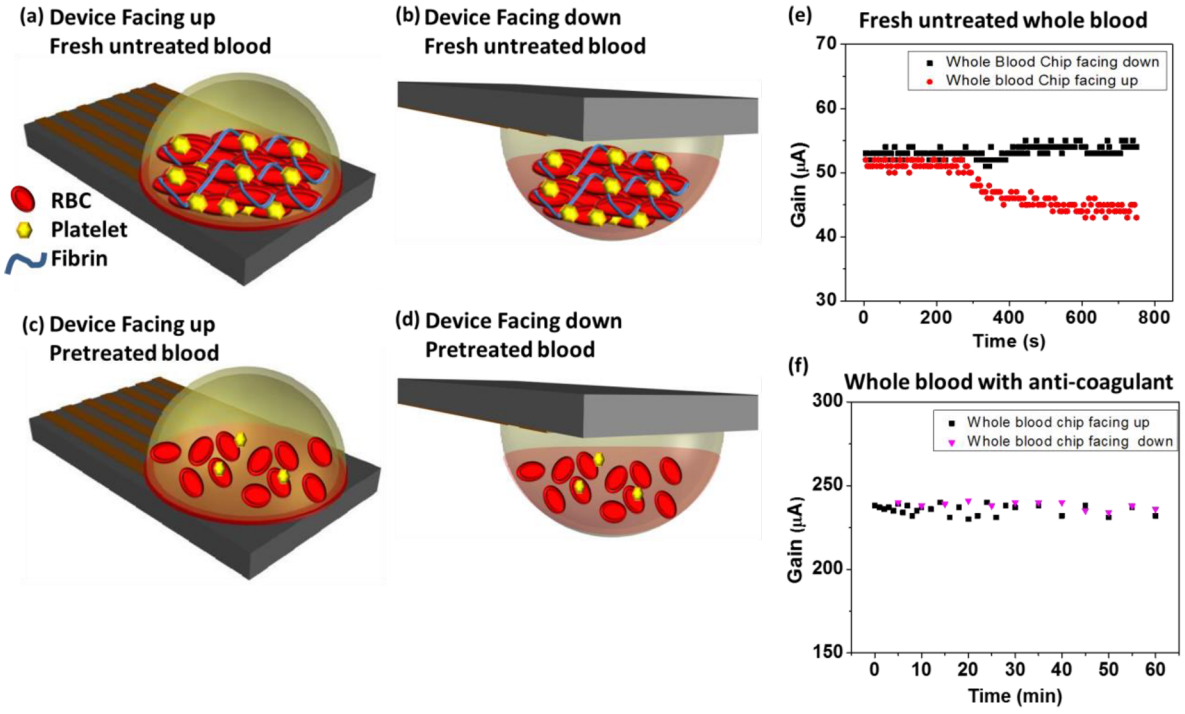

Figure 2. Electrical characteristics of whole blood on sensor surface. (a, b) Untreated blood dropped on the device facing up and down, respectively. (c, d) Pretreated (anticoagulated) blood dropped on the device facing up and down, respectively. (e, f) Electrical response of the sensor with untreated and pretreated (anticoagulated) whole blood, respectively.

FET sensor is shown in Figure 1a, and the top view image is shown in Figure 1b. The open areas on the pair of gold electrodes which are separated by a fixed gap are regarded as the sensing region of the extended gate FET sensor.

For whole blood testing, venous blood samples are collected. A single drop of blood sample is dropped on the sensor chip, and the chip is upturned and held in the downward facing position for 5 min. After the incubation period, electrical measurement is carried out using the portable biosensor system and results are displayed on the computer interfaced with the system. The assay protocols are illustrated in Figure S3. No additional protocols are required for carrying out the whole blood testing.

When test solution is dropped on the sensing region and biased with a pulsed gate voltage, the applied potential drops across the test solution, instantly creating an electrical double layer on the interfaces of the reference gate electrode and sensing electrodes, setting up a solution capacitance C_s. Since the sensing electrode is connected to the MOSFET, the applied potential also drops across the gate oxide dielectric of the MOSFET, which leads to a change in the transistor channel conductivity. Therefore, the applied gate voltage V_g drops across the solution and the gate oxide, modulating the transistor drain current, as shown in eq 1.

$$V_g = \Delta V_s + \Delta V_{ox} \tag{1}$$

Where V_g is the applied gate bias and V_s and V_{ox} are the potential drops across the solution and the MOSFET gate oxide, respectively.

The potential drop across the test solution, V_s, which creates the solution capacitance, C_s, modulates the potential drop across the gate oxide of the MOSFET. In an electrical circuit, the impedance is described by eq 2 and the total capacitance in a series circuit, by eq 3.

$$Z = \frac{1}{j\omega C} \tag{2}$$

$$\frac{1}{C_{total}} = \frac{1}{C_1} + \frac{1}{C_2} + \cdots + \frac{1}{C_n} \tag{3}$$

Therefore, following eqs 1, 2, and 3, the effective potential drop across the MOSFET gate oxide can be described by eq 3 as

$$\Delta V_{ox} = \frac{\frac{1}{j\omega C_{ox}}}{\frac{1}{j\omega C_{ox}} + \frac{1}{j\omega C_s}} \times V_g = \frac{C_s}{C_{ox} + C_s} \times V_g \tag{4}$$

where C_s and C_{ox} are the solution capacitance and the oxide capacitance, respectively, which are connected in series circuit, j is complex function, and ω is angular frequency.

From eq 4, we can infer that potential drops across the solution and the gate oxide, which creates C_s and C_{ox}, respectively, modulates the transistor drain current. When the ion concentration in the test solution increases, the solution capacitance C_s increases, which increases the potential drop in the gate oxide V_{ox} and hence the transistor drain current. This means that, in high ionic strength solutions such as 1× PBS or physiological fluids such as whole blood, C_s increases, leading to an increase in transistor drain current. Thus, the sensor gating mechanism can overcome the limitations of charge screening in traditional FET-based biosensors because the high field applied to the sensor via the reference gate electrode-sensing electrode pair can modulate the channel drain current. As seen in eq 4, this type of sensor is indeed an ion gated or EDL gated high field FET biosensor. Throughout this study, we do not rely on the absolute transistor drain current (I_D) but the difference in drain current before and after applying gate voltage (ΔI_D). The ΔI_D is denoted as current gain or simply gain of the FET, synonymous to transconductance gain g_m of traditional

DOI: 10.1021/acs.analchem.7b05018
Anal. Chem. 2018, 90, 2867−2874

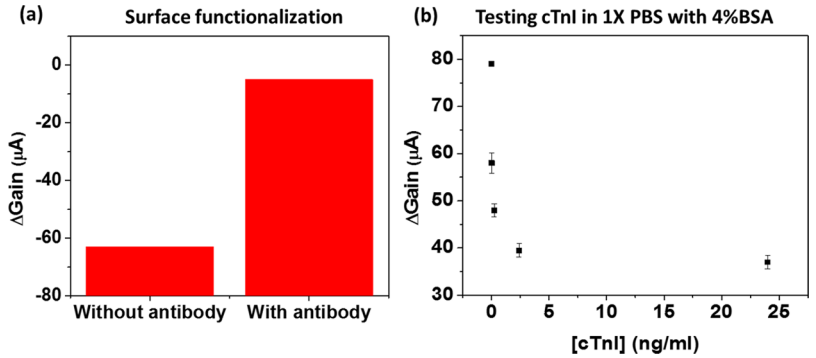

Figure 3. Sensor characteristics in 1× PBS with 4% BSA. Sensor response is noted as the differential current gain which is defined as the difference of current gain of gold electrodes with and without antibody. (a) The change in sensor response upon surface functionalization. (b) Calibration curve for cTnI detection in 1× PBS with 4% BSA.

MOSFET. Current gain is preferred over the absolute drain current as sensor signal because absolute I_D is more prone to variations due to thermal noise and external impedance loading effects. On the other hand, current gain ΔI_D which is the difference in drain current before and after applying V_g is a more stable and consistent sensor index.

Sensor Response in Whole Blood. The electrical characteristics of testing whole blood samples is shown in Figure 2. Human blood consists of one-half of a liquid portion containing proteins and another half of blood cells such as red blood cells (RBCs), white blood cells (WBCs), and platelets. Blood cells possess the ability to form highly contracted and dense clots. In this study, we have investigated two types of blood samples: fresh, untreated whole blood samples and pretreated whole blood samples (containing anticoagulant). Figure 2a–d shows the schematic representation of conditions used to test whole blood samples and the effect of whole blood on the sensor chip. When untreated blood is dropped on the sensor surface, it starts to coagulate in 4–5 min. On the other hand, the pretreated blood samples do not coagulate due to the presence of anticoagulants. However, the blood cells can still sediment to the bottom because of gravity. Figure 2a shows the blood clot formation in the droplet of untreated whole blood sample dropped on the sensor chip which is held in a downward facing position. A blood clot is a highly dense collection of RBCs which is encapsulated in a mesh of platelets and insoluble fibrin strands. The clot quickly settles to the bottom along the force of gravity. On the other hand, as seen in Figure 2b, when the droplet of pretreated whole blood sample is dropped on the sensor which is then held in a downward facing position, the blood cells do not form a close packing as observed in blood clots but, eventually, settle to the bottom, acting along the force of gravity. The sedimented blood cells are not closely packed together and have loose intercellular junctions. In Figure 2c, the schematic represents the effect of dropping untreated whole blood sample on the sensor chip which is held in an upward facing position. The blood cells coagulate and form a dense blood clot which settles to the bottom, on to the sensor surface. When pretreated whole blood sample is dropped on the sensor chip held in an upward facing position, the blood cells sediment to the surface of the sensor, as shown in Figure 2d. In this case, the blood cells, that sediment at the bottom, do not form a dense aggregate. Instead, they have loose intercellular junctions (like in Figure 2b) and very weak or no adhesions to the sensor surface. The electrical response of sensor in the above listed scenarios is depicted in Figure 2e,f. As seen in Figure 2e, when untreated whole blood sample is tested, the sensor signal remains steady for the duration of the test, when the chip is facing downward. The formation of a blood clot and its sedimentation does not significantly affect the sensor response. In contrast, when the chip is facing upward, the current gain of the sensor decreases, indicating the physical changes related to the clotting process within the droplet of blood. On the contrary, when pretreated blood sample is dropped on the sensor surface, as in Figure 2f, the electrical response of the sensor does not show significant changes, when the sensor is facing upward or downward. This means that, although the blood cells sediment to the bottom, the applied electric field can still drop across the solution and reach the gate oxide of MOSFET and modulate the channel conductivity.

Purified cTnI Detection in 1× PBS with 4% BSA. Figure 3 describes the characteristics of cTnI detection in 1× PBS with 4% BSA. cTnI specific monoclonal antibody is used as the receptor to capture cTnI present in the test solution. The reference gate electrode is functionalized with the antibody as described in the Methods section, and the immobilization of antibody can be verified electrically. Figure 3a depicts the change in sensor signal after antibody immobilization. When antibody is immobilized, or target protein is bound to the antibody, the charge distribution in the local region of the EDL changes, which effectively changes C_s.[25] Thus, the change in C_s can modulate the V_{ox} and hence current gain of the sensor. In Figure 3, the y axis is differential gain, which is the difference of current gain of gold electrodes with and without immobilized antibody (gain of sensing gold electrodes minus gain of bare gold electrode). This differential gain is a useful sensor index as it can dynamically monitor the changes in the solution capacitance with respect to the bare gold electrode, for each individual droplet of test solution, whereby eliminating any variations originating from external sources such as temperature and humidity of test environment, fluid pressure, droplet consistency, and surface energy. After verifying the antibody immobilization, the sensor is used to test for cTnI prepared in 1× PBS with 4% BSA. The reason for adding 4% BSA in buffer is to mimic the physiological conditions of human serum in which albumin is the most abundant protein. Figure 3b shows the calibration curve for cTnI detection in 1× PBS with 4% BSA. The cTnI values tested are 0 (1× PBS with 4% BSA), 0.024, 0.24, 2.4, and 24 ng/mL. When the cTnI concentration increases, the current gain of the FET sensor decreases. The sensor exhibits very high sensitivity in high salt concentration

DOI: 10.1021/acs.analchem.7b05018
Anal. Chem. 2018, 90, 2867–2874

and can detect cTnI over a wide dynamic range, which is relevant to the clinical concentration range of cTnI. The results in Figure 3b demonstrate that the sensor can directly detect cTnI in physiological salt concentrations, without suffering from the drawbacks of charge screening or interference due to high concentration of background proteins such as albumin.

Purified cTnI Detection in Whole Blood. In Figure 4, the sensor characteristics of detection of cTnI in whole blood samples are elucidated. The whole blood sample used to perform this experiment is treated with anticoagulant. The cTnI concentration in the blood samples is predetermined to be less than the detection limit of the laboratory instrument. The whole blood sample is then spiked with different concentrations of cTnI ranging from 0.024 to 24 ng/mL. Figure 4 shows the calibration curve for testing cTnI in spiked whole blood samples. The cTnI values tested are 0 (undetected cTnI in blood), 0.024, 0.24, 2.4, and 24 ng/mL. The inset graph shows the calibration curve in log scale, to demonstrate the linearity of the sensor. The current gain of the sensor decreases in a concentration dependent manner, as was observed in the detection of purified cTnI samples (Figure 3b). The results depicted in Figure 4 demonstrate the capability of the extended gate EDL FET sensor to directly detect target protein in whole blood samples, without any extensive sample pretreatments such as dilution, desalting, or filtering. The sensor also demonstrates high sensitivity and wide dynamic range (0−24 ng/mL) which are important sensor characteristics for clinical diagnostics.

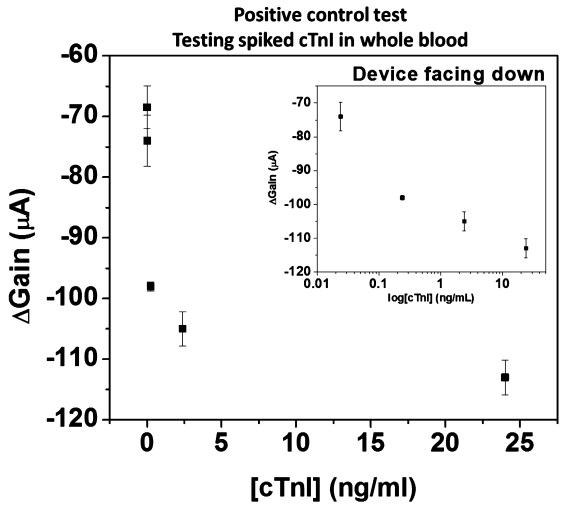

Figure 4. Sensor characteristics in whole blood samples spiked with cTnI. The cTnI concentrations in the whole blood samples are 0 (undetected cTnI), 0.024, 0.24, 2.4, and 24 ng/mL.

cTnI Detection in Clinical Whole Blood. Figure 5 shows the results of testing clinical whole blood samples obtained from patients admitted to the hospital due to relevant symptoms of cardiac distress. The cTnI values in the blood samples have been determined using standard laboratory equipment. Figure 5a,b depicts the sensor calibration curves for cTnI detection in clinical whole blood samples, for sensor chip facing downward and upward, respectively. The cTnI values tested are 0.08, 0.75, 1.94, 7.64, 12.52, 14.51, and 16.59 ng/mL. The current gain decreases in a concentration dependent manner in both cases, which agrees with the data provided in Figures 3 and 4. The current gain of bare electrodes will not vary consistently (as the sensing electrode), because it is not functionalized with receptor. Therefore, when the difference of gain values of the sensor and bare gold electrodes is taken, the *y* axis may have negative values, as seen in Figure 5. The electrical response of the sensor is not significantly affected by the sedimentation of blood cells in the anticoagulated whole blood samples. The sensors exhibit high sensitivity and wide dynamic range of detection of cTnI (0.08−16.59 ng/mL). More importantly, the whole blood samples are obtained from different patients, at different times, yet the sensor response follows the concentration dependent trend which is observed in purified cTnI samples and spiked whole blood samples. This means that the interference from nonspecific signals arising from patient to patient blood sample variations does not severely impede the electrical characteristics of our sensor.

The sensor is washed in mild protein elution buffer and 1× PBS to remove any nonspecific binding on the sensor surface. The protein elution protocols and electrical test results of sensor regeneration are detailed in Figure S4. Each test solution sample is dropped on the sensor and incubated for 5 min before recording the current gain. During this time, the specific binding, which is the antibody−antigen binding, achieves steady state and dominantly contributes to the change in electrical signal, and the nonspecific binding is relatively very low. This is because nonspecific binding typically has a much lower reaction rate as opposed to specific antibody−antigen binding. Nonetheless, between each cTnI concentration test, the sensor surface is regenerated by eluting the bound cTnI and other background proteins and cells away. In this way, during every test, we can control the background response, by keeping the

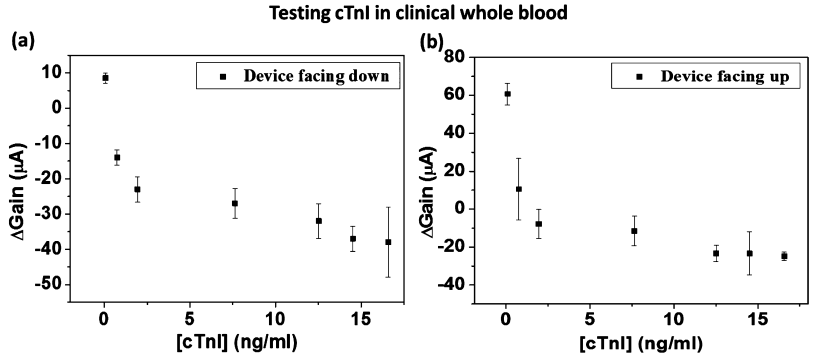

Figure 5. Sensor characteristics in clinical whole blood samples. Calibration curve for cTnI detection in clinical whole blood samples with (a) the device facing down and (b) the device facing up. The cTnI values in the blood samples are 0.08, 0.75, 1.94, 7.64, 12.52, 14.51, and 16.59 ng/mL.

DOI: 10.1021/acs.analchem.7b05018
Anal. Chem. 2018, 90, 2867−2874

nonspecific binding to a bare minimum. In both cases (device facing upward and downward), the accumulation of blood cells or background proteins does not cause interference in testing, as we can see that the sensor surface can be cleaned effectively (Figure S4), using the protein elution−washing procedure.

DISCUSSION

One of the major concerns in a protein detection assay using whole blood samples is the interference from blood cells which make up about half the volume of blood. Previously, label free, protein detection from whole blood was achieved by the means of a complex microfluidic purification chip followed by detection using the FET biosensor.[23] However, it is not a practical approach toward designing a low cost, in vitro diagnostic assay for rapid protein biomarker screening. In another study using DNA-based electrochemical sensor, protein detection in whole blood has been demonstrated.[26] However, such a sensing method would require additional labeling reagents and is not applicable for all types of immunoassays. In our study, the purpose of holding the sensor chip in a downward facing position during the incubation period is to gravitationally separate blood cells from the plasma to minimize their interference. In fresh, untreated blood samples, blood clots are formed in 4−5 min which settle to the bottom with an increased terminal velocity compared to normal cells.[27] In this way, when the sensor chip is facing downward, the blood cells can be quickly and efficiently separated from the plasma. Accordingly, when the device is facing upward, the blood clots, which are highly contractible and dense, settle on the sensor surface which leads to a decrease in sensor signal. Interestingly, while using pretreated whole blood samples (containing anticoagulant), electrical results shown in Figures 2f and 5b demonstrate that the sensor response is not adversely affected by the sedimentation of blood cells, even with the device facing upward configuration. This can be explained by the overall change in impedance of coagulated and anticoagulated blood and from the morphological shape of the blood cells. Electrical impedance is a method that is commonly used in hematology analyzers in hospitals today.[28] Previous studies have reported that the electrical impedance of blood samples increases upon clot formation and the change in impedance is used to dynamically monitor the blood clotting process.[29−31] It is also shown that, when the concentration of anticoagulant is increased, and hematocrit is decreased, the impedance of whole blood decreases.[31,32] This confirms that a larger blood clot contributes toward larger impedance. However, that does not fully explain the electrical results obtained using our FET sensor. Electrical impedance sensors that study the interaction of cells to the substratum and neighboring cells have been reported previously.[33,34] In these studies, it has been reported that when the confluence of cells on the substrate increases, the electrical impedance increases. This is attributed to the decreasing cell to substrate distance and tight intercellular junctions, which increases the electrical impedance. The cell−cell adhesion is significantly increased during coagulation which leads to tight intercellular junctions and higher density of coagulated cells.[27] The change in morphology of RBCs from discoid to polyhedral, revealed in a recent study,[35] suggests the decreased cell−substrate distance during coagulation. In another study, it has been shown that, with increasing adhesion and spreading of cells on the substrate, the ions within the EDL are displaced, leading to an increase in electrical impedance.[36,37] When our sensor is facing up, in untreated blood samples, clot formation occurs which is highly dense and compact. This can be viewed as the scenario of increased adhesion to the sensor substrate, as the drag force acting on the highly dense blood clot is higher than normal cells. Therefore, the sensor signal decreases due to increased impedance. On the other hand, in pretreated blood, the blood cells sediment on the sensor surface (when it is facing upward) but do not clot. This can be viewed as poor adhesion to the sensor surface with loose intercellular junctions and comparatively less electrical impedance. This can explain why our sensor response is not significantly affected by the presence of blood cells on the sensor surface, in pretreated blood samples. Although the electrical results are quite convincing, it may still be preferred to perform the electrical testing with the sensor chip facing downward in order to gravitationally separate the blood cells from plasma, to avoid any interference, however minor it may be, from affecting the test results. By doing so, the end user still does not need to perform any additional assay protocol, thereby not compromising on the simplicity and robustness of the assay.

The results shown in Figures 4 and 5 not only display high sensitivity and wide dynamic range of detection but also demonstrate the specificity of the sensor to the target protein. The whole blood sample used in the experiment contains several background proteins which are present in large quantities, several orders of magnitude higher than the target protein concentration. However, the sensor signal is a concentration dependent curve, which can be attributed to the very less sample incubation period required (5 min) and to the sensor mechanism. In this sensor, when the target protein undergoes specific binding with the receptor, local charge distribution within the EDL changes which influences the solution capacitance C_s and hence modulates the channel conductivity. The background proteins on the other hand do not have sufficient time to develop strong electrostatic interactions which leads to almost no change in sensor response. This gives rise to specificity of sensor toward target protein. This is also preserved in testing clinical whole blood samples, which are obtained from different patients. Every individual will have slight variations in their blood samples, in the levels of metabolites, cell counts, clotting factors, and serum proteins. Results shown in Figure 5 show that the sensor can still respond with a target protein concentration dependent curve, demonstrating specificity across different whole blood samples from different patients. However, the sensitivity in higher concentrations of cTnI (around 20 ng/mL) is lower than that in low concentrations. This is primarily due to the high affinity of the receptor to the target. The sensing characteristics can be improved by using a combination of antibodies with K_D values in low and high concentrations of cTnI to obtain a linear response over a wide dynamic range.

CONCLUSION

The extended gate design of the EDL FET sensor used in this study has several advantages. The sensing region is located on the detachable and replaceable sensor array chip consisting of gold electrode pairs which is connected to the MOSFET. In this way, a single FET can be used to test several sensor array chips which reduces the variations arising from FET to FET sensor and brings down the cost even further. It may even be used in a "disposable after use" fashion. This is of importance as a point of care or mobile diagnostic device, as reliability and affordability are the major concerns in such systems. More importantly, this method of biomolecule detection can be

DOI: 10.1021/acs.analchem.7b05018
Anal. Chem. 2018, 90, 2867−2874

extended to all types of FETs including commercial MOSFETs such as the one used in this study, compound semiconductor-based FETs with unique electrical properties and novel 2-dimensional material-based FETs which can offer extremely high sensitivities. Since the biological solution does not touch the FET, there arises no issues of biocompatibility of FET or drift in electrical response. Thus, the combination of gold electrode pair and FET can be used to detect any biomolecule via molecular recognition assay. Gravitational separation of blood cells in whole blood samples is adopted to easily avoid any interference from blood cells. It is also demonstrated that, if clot formation is prevented using anticoagulants, gravitational separation is unnecessary, as the sensor response is not adversely affected by the accumulated cells. The test results in purified cTnI samples prepared in 1× PBS with 4% BSA, whole blood samples spiked with purified cTnI, and clinical whole blood samples demonstrate very high sensitivity and specificity and a wide dynamic range of detection. We believe this sensing methodology can revolutionize the point of care and mobile diagnostics industry, better the prospects of affordable health monitoring assays, radically bring down the cost of commercial diagnostics, and shorten the time between diagnosis and medical intervention.

■ ASSOCIATED CONTENT

Supporting Information

The Supporting Information is available free of charge on the ACS Publications website at DOI: 10.1021/acs.analchem.7b05018.

Fabrication of sensor array chip; sensor measurement; immunoassay protocols; sensor regeneration (PDF)

■ AUTHOR INFORMATION

Corresponding Authors

*E-mail: ylwang@mx.nthu.edu.tw.
*E-mail: drlawrenceliu@gmail.com.

ORCID

Yu-Lin Wang: 0000-0002-4791-936X

Author Contributions

Y.-L.W. guided the whole sensor works and edited this Article. L.Y.-M.L. provided whole blood samples and support in sample handling and discussions. H.-H.K.C. provided valuable suggestions and support in the development of this work. I.S. designed, fabricated, and characterized the sensor and conducted data analysis. S.-L.W., R.S., and P.-C.C. took measurements and assisted with analysis. T.-Y.D. and A.K.P. assisted with material preparation, device fabrication, and process discussions. C.-P.H. aided in portable sensor system design.

Notes

The authors declare no competing financial interest.

■ ACKNOWLEDGMENTS

This work was partially supported by research grants from Ministry of Science & Technology (MOST 106-2221-E-007-002; MOST 106-2218-E-007-015-MY2), NTHU-Hsinchu Mackay Memorial Hospital 2017 joint project, National Yang-Ming University (2017 SPARK), and National Tsing Hua University (106N523CE1). We are thankful for the technical support from National Nano Device Laboratories (NDL) in Hsinchu and the Center for Nanotechnology, Materials Science, and Microsystems (CNMM) at National Tsing Hua University.

■ REFERENCES

(1) Walsh, J. A.; Topol, E. J.; Steinhubl, S. R. *Circulation* **2014**, *130*, 573−581.
(2) Fung, E.; Järvelin, M.-R.; Doshi, R. N.; Shinbane, J. S.; Carlson, S. K.; Grazette, L. P.; Chang, P. M.; Sangha, R. S.; Huikuri, H. V.; Peters, N. S. *Front. Physiol.* **2015**, *6*, 149.
(3) Drew, B. J.; Califf, R. M.; Funk, M.; Kaufman, E. S.; Krucoff, M. W.; Laks, M. M.; Macfarlane, P. W.; Sommargren, C.; Swiryn, S.; Van Hare, G. F.; American Heart Association; Councils on Cardiovascular Nursing, Clinical Cardiology, and Cardiovascular Disease in the Young. *Circulation* **2004**, *110*, 2721−2746.
(4) Boldt, J. *Critical Care* **2002**, *6*, 52−59.
(5) Benjamin, E. J.; Blaha, M. J.; Chiuve, S. E.; Cushman, M.; Das, S. R.; Deo, R.; de Ferranti, S. D.; Floyd, J.; Fornage, M.; Gillespie, C.; Isasi, C. R.; Jiménez, M. C.; Jordan, L. C.; Judd, S. E.; Lackland, D.; Lichtman, J. H.; Lisabeth, L.; Liu, S.; Longenecker, C. T.; Mackey, R. H. *Circulation* **2017**, *135*, e146.
(6) Gersh, B. *Circulation* **2012**, *126*, A606.
(7) Suzuki, T.; Nagai, R. *Nat. Clin. Pract. Cardiovasc. Med.* **2008**, *5*, 295.
(8) Ge, Y.; Wang, T. J. *J. Intern. Med.* **2012**, *272*, 430−439.
(9) Neumann, J.; Sörensen, N.; Schwemer, T.; et al. *JAMA Cardiology* **2016**, *1*, 397−404.
(10) Mythili, S.; Malathi, N. *Biomed. Rep.* **2015**, *3*, 743−748.
(11) Song, S. Y.; Han, Y. D.; Kim, K.; Yang, S. S.; Yoon, H. C. *Biosens. Bioelectron.* **2011**, *26*, 3818−3824.
(12) Zhang, L.; Xiong, C.; Wang, H.; Yuan, R.; Chai, Y. *Sens. Actuators, B* **2017**, *241*, 765−772.
(13) de Winter, R. J.; Koster, R. W.; Sturk, A.; Sanders, G. T. *Circulation* **1995**, *92*, 3401−3407.
(14) Masson, J.-F.; Battaglia, T. M.; Khairallah, P.; Beaudoin, S.; Booksh, K. S. *Anal. Chem.* **2007**, *79*, 612−619.
(15) Allen, B. L.; Kichambare, P. D.; Star, A. *Adv. Mater.* **2007**, *19*, 1439−1451.
(16) Kaisti, M. *Biosens. Bioelectron.* **2017**, *98*, 437−448.
(17) Chen, K.-I.; Li, B.-R.; Chen, Y.-T. *Nano Today* **2011**, *6*, 131−154.
(18) Ren, F.; Pearton, S. J. *physica status solidi (c)* **2012**, *9*, 393−398.
(19) Wang, C.; Cui, X.; Li, Y.; Li, H.; Huang, L.; Bi, J.; Luo, J.; Ma, L. Q.; Zhou, W.; Cao, Y.; Wang, B.; Miao, F. *Sci. Rep.* **2016**, *6*, 21711.
(20) Sarkar, D.; Liu, W.; Xie, X.; Anselmo, A. C.; Mitragotri, S.; Banerjee, K. *ACS Nano* **2014**, *8*, 3992−4003.
(21) Shoorideh, K.; Chui, C. O. *Proc. Natl. Acad. Sci. U. S. A.* **2014**, *111*, 5111−5116.
(22) Elnathan, R.; Kwiat, M.; Pevzner, A.; Engel, Y.; Burstein, L.; Khatchtourints, A.; Lichtenstein, A.; Kantaev, R.; Patolsky, F. *Nano Lett.* **2012**, *12*, 5245−5254.
(23) Stern, E.; Vacic, A.; Rajan, N. K.; Criscione, J. M.; Park, J.; Ilic, B. R.; Mooney, D. J.; Reed, M. A.; Fahmy, T. M. *Nat. Nanotechnol.* **2010**, *5*, 138−142.
(24) Zheng, G.; Patolsky, F.; Cui, Y.; Wang, W. U.; Lieber, C. M. *Nat. Biotechnol.* **2005**, *23*, 1294.
(25) Chu, C.-H.; Sarangadharan, I.; Regmi, A.; Chen, Y.-W.; Hsu, C.-P.; Chang, W.-H.; Lee, G.-Y.; Chyi, J.-I.; Chen, C.-C.; Shiesh, S.-C.; Lee, G.-B.; Wang, Y.-L. *Sci. Rep.* **2017**, *7*, 5256.
(26) Mahshid, S. S.; Camiré, S.; Ricci, F.; Vallée-Bélisle, A. *J. Am. Chem. Soc.* **2015**, *137*, 15596−15599.
(27) Fogelson, A. L.; Neeves, K. B. *Annu. Rev. Fluid Mech.* **2015**, *47*, 377−403.
(28) Davis, B. H.; Barnes, P. W. In *Laboratory Hematology Practice*; Wiley-Blackwell: Hoboken, NJ, 2012; pp 26−32.
(29) Ur, A. *Nature* **1970**, *226*, 269−270.
(30) Ur, A. *Am. J. Clin. Pathol.* **1977**, *67*, 470−476.
(31) Lei, K. F.; Chen, K.-H.; Tsui, P.-H.; Tsang, N.-M. *PLoS One* **2013**, *8*, e76243.

DOI: 10.1021/acs.analchem.7b05018
Anal. Chem. 2018, 90, 2867−2874

(32) Berney, H.; O'Riordan, J. J. *Impedance measurement monitors blood coagulation*, 2008; Vol. *42*; http://www.analog.com/cn/analog-dialogue/articles/impedance-measurement-monitors-blood-coagulation.html.
(33) Giaever, I.; Keese, C. R. *Proc. Natl. Acad. Sci. U. S. A.* **1991**, *88*, 7896−7900.
(34) Lo, C. M.; Keese, C. R.; Giaever, I. *Biophys. J.* **1995**, *69*, 2800−2807.
(35) Cines, D. B.; Lebedeva, T.; Nagaswami, C.; Hayes, V.; Massefski, W.; Litvinov, R. I.; Rauova, L.; Lowery, T. J.; Weisel, J. W. *Blood* **2014**, *123*, 1596.
(36) Svetličić, V.; Ivošević, N.; Kovač, S.; Žutić, V. *Bioelectrochemistry* **2001**, *53*, 79−86.
(37) Svetličić, V.; Ivošević, N.; Kovač, S.; Žutić, V. *Langmuir* **2000**, *16*, 8217−8220.

DOI: 10.1021/acs.analchem.7b05018
Anal. Chem. 2018, 90, 2867−2874